Research Article | Vol. 29, No. 18 / 30 Aug 2021 / Optics Express 29357
Optics EXPRESS

Performance enhancement of an ultrafast all-fiber laser based on an InN saturable absorber using GRIN coupling

L. MONROY,[1,*] M. SORIANO-AMAT,[1] Ó. ESTEBAN,[1] E. MONROY,[2] M. GONZÁLEZ-HERRÁEZ,[1] AND F. B. NARANJO[1]

[1] *Grupo de Ingeniería Fotónica, Dept. Electrónica (EPS) Universidad de Alcalá, Campus Universitario Alcalá de Henares 28871, Madrid, Spain*
[2] *Univ. Grenoble-Alpes, CEA, Grenoble INP, IRIG, PHELIQS, 17 av. des Martyrs, 38000 Grenoble, France*
[*] *laura.monroy@uah.es*

Abstract: Indium nitride (InN)-based semiconductor saturable absorbers have previously shown advantages for application in near-IR fiber lasers due to their broad modulation depth, ultrafast nonlinear response and thermal stability. However, up to now all demonstrated saturable absorber elements based on InN (either transmissive or reflective) have shown limited performance due to poor coupling and insertion losses. We present here a simple mode-locking device based on a GRIN-rod lens in conjunction with an InN semiconductor saturable absorber mirror (SESAM) for its use in a passively mode-locked all-fiber laser system operating at telecom wavelengths. Our results demonstrate that this coupling element ensures not only a compact, turnkey and alignment-free design but also a highly-stable optical femtosecond pulse train. The reduction of insertion losses (3.5 dB) enables the generation of 90-fs ultrafast pulses with an average power of 40 mW and up to 7 nJ of pulse energy without the need for additional amplification.

1. Introduction

Laser sources generating ultrafast optical pulses are currently on demand as essential tools for many industrial, medical and military applications, such as material processing, micromachining, surgery and telecommunications [1–4]. In the past decade, ultrafast fiber laser technologies have been extensively investigated owing to their inherent properties including potentially alignment-free operation, environmental robustness and low cost. The flexibility and stability of such sources enable them to produce high peak power pulses in the picosecond and femtosecond regimes [5]. The industrial growth of the ultrafast fiber laser market has been strongly accelerated by the use of active (e.g. using an electro-optic modulator) [6,7] or passive (e.g. inserting a saturable absorber) [8,9] mode-locking techniques. Comparing both approaches, passively mode-locked fiber laser schemes have the advantages of simplicity, compactness and shorter achievable pulse durations. The passive approach is based on the use of a nonlinear optical element, which turns the continuous-wave (CW) lasing into a train of ultrashort optical pulses. In order to achieve passive mode-locking in a fiber laser, several techniques can be employed, such as nonlinear polarization rotation (NPR) [10], nonlinear loop mirrors (NOLM or NALM) [11] or saturable absorbers (SA) [8]. Both NOLM and NALM techniques can provide sub-100 fs pulses in a self-starting configuration, with the use of polarization maintaining fibers (PM) and nonreciprocal phase-shifter components [12]. Saturable absorbers constitute one of the most extended optical components for ultrafast pulse generation due to their efficiency, stability and low cost. In this case, the energy and stability of stretched pulses are limited not only by the net dispersion (excessive nonlinearities may cause optical wave-breaking) but also by the SA parameters; i.e. modulation depth, recovery time, etc. Therefore, efficient SAs with large

#430198 https://doi.org/10.1364/OE.430198
Journal © 2021 Received 19 May 2021; revised 9 Aug 2021; accepted 10 Aug 2021; published 26 Aug 2021

Optics EXPRESS

modulation depth and high-power tolerance are required for passively mode-locked ultrafast pulse generation.

Among SAs for passive mode-locking, semiconductor saturable absorber mirrors (SESAM) are one of the most relevant technologies, particularly in industrial-grade ultrafast mode-locked and solid-state lasers operating at 1 µm and 1.5 µm [13]. Depending on their chemical composition, SESAMs can now cover a large spectral range and exhibit strong nonlinearities and are hence employed in applications requiring high-resolution and time-resolved measurements. However, SESAMs require sophisticated manufacturing processes and have some limitations: they are often narrowband (few nm bandwidth) devices with a low damage threshold and long recovery times (picosecond or nanosecond range). Therefore, the exploration of SAs with superior properties still remains a challenge.

In recent years, new types of saturable absorbers based on 2D materials have been tested in many applications (nonlinear optics [14], microelectronic devices [15], biomedicine [16]) due to their advantages in terms of controllable modulation depth, ultrafast recovery time and easy fabrication. In this sense, several 2D materials, such as graphene [17,18], topological insulators [19], transition dichalcogenides [20], and black phosphorus [21,22], have emerged as efficient fiber SAs. Also, many researchers have focused their attention on newly monoelemental materials including phosphorene [23], antimonene, arsene, and bismuthine [24], with attractive parameters such as broadband operation, low saturation fluence and fast recovery time. However, some restrictions (low damage threshold or the required fine-controlled monolayer deposition) have hindered the commercial implantation of these technologies.

A simple and cost-effective alternative relies on the use of indium nitride (InN) thin films, which have demonstrated high-thermal and chemical stability (high fluence tolerance), polarization insensitivity, and extremely high optical nonlinearities [25,26]. The operating band gap of this technology is reported to be around 0.65 eV to 0.9 eV, thus working in the telecommunication region [27]. All these characteristics make InN a promising candidate as saturable absorber for commercial applications.

Recently, we have proposed and demonstrated the use of InN thin films (presenting a smooth surface morphology with atomic terraces with a residual carrier concentration below 10^{18} cm^{-3}, a band gap energy = 0.67 eV and a linear absorption coefficient of 4×10^4 cm^{-1}). In relation to the nonlinear properties, the InN materials demonstrate a nonlinear absorption coefficient of -3×10^4 cm/GW) as saturable absorbers with high modulation depth (23%) and nonlinear transmission change (715%) measured with the Z-scan technique as mentioned in Ref. [27]. Subsequently, a passively mode-locked fiber laser using InN SESAMs in free-space configuration was demonstrated, delivering highly stable ultrashort pulses with a pulse width of 134 fs at 1560 nm with an energy per pulse of 5.4 nJ [28]. However, the use of free-space optics in the SESAM yielded relatively high intracavity losses and therefore performance degradation, estimated in 8,5 dB of insertion losses.

The demand for alignment-free, high-power ultrafast lasers has led to the development of new fabrication methods for all-fiber systems, based on the deposition of the SA onto the optical fiber. Most often SAs are transferred by spin coating on transparent plates or highly reflective mirrors [29], keeping a free-space configuration of the laser cavity. An alternative configuration consists of inserting the SA between two fiber ends with a connector (butt-coupling) [30]. The SA material is glued to the fiber facet using a composite material, e.g. organic polyvinyl alcohol (PVA) or polymethyl methacrylate. Although this method is relatively simple and can be used in commercial systems with any type of fiber connector, it also presents some disadvantages, such as low damage threshold which limits its application for high-power ultrafast fiber lasers. To solve these limitations, an evanescent-wave coupling was proposed. The laser light would leak out of the fiber core and interact with the SA deposited on the sidewalls of the optical fiber, i.e., tapered fibers [31], side-polished fibers [32], or cladding-etched fibers [33]. However, these

Optics EXPRESS

types of fibers induce nonlinear polarization rotation effects in the laser cavity, hence reducing the optical peak power. Recently, new fiber lasers based on ultra-long-period gratings have been demonstrated, generating output soliton pulses with up to 8.4 mW of average power and 7.8 ps pulse-width [34]. Therefore, new coupling methods are essential for high-power ultrafast fiber lasers.

In this paper we present a simple, alignment-free, all-fiber laser device using an InN SESAM and a GRIN lens as a coupling device to reduce the SA insertion losses. In our scheme, the InN-based device is glued to the fiber facet with a UV-curing optical adhesive. In order to increase the nonlinear response of the SA, a GRIN rod-lens has been incorporated between the optical fiber and the SA as shown in Fig. 1(a). Both optical elements are glued directly to the lens faces with the transparent cement. The resulting solid assembly has no optical path in air, which reduces the reflection losses at interfaces and the optical aberrations due to the lenses, which ultimately leads to narrower laser pulses and higher output power. We demonstrate that the optical pulses can be as short as 90 fs, and the peak power and energy of the output pulses can reach 74 kW and 8 nJ, respectively. These values are higher than those describing the best 2D material performance. As it can be seen from the results, an enhancement of the ultrafast laser performance is achieved by inserting a simple GRIN-to-fiber coupling device in between the fiber end and the InN based SESAM. This coupling device (GRIN with InN SESAM) demonstrated high damage threshold, polarization insensitivity and low insertion losses in comparison to the aforementioned coupling methods. These results pave the way for commercial ultrafast all-fiber laser assemblies in the telecommunication region based on InN.

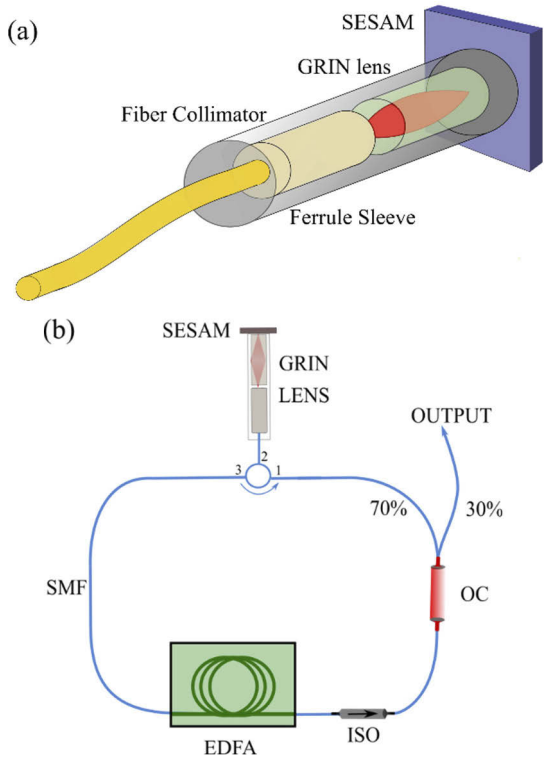

Fig. 1. System design and components: (a) fiber integration of the saturable absorber by material deposition on the fiber end with a GRIN-rod lens, and (b) block diagram of the all-fiber Er-doped laser emitting at 1.56 µm.

Optics EXPRESS

2. Laser setup and experimental results

The experimental setup of the fiber laser is depicted in Fig. 1(b). The GRIN lens is a commercially-available lens (GRIN2315, Thorlabs with a focal distance of 0.245 mm and a plain and broadband response over the spectral range of the optical laser is measured, 100 nm around its central wavelength 1550 nm). The GRIN lens has a transmittance of 90% from 380 to 2000nm and a total polarization preservation., which enables its use for industrial applications. The SA is an InN epitaxial layer deposited on a commercial GaN-on-sapphire substrate by plasma-assisted molecular beam epitaxy (MBE) at a growth temperature of 450°C and with a growth rate of 290 nm/h. In order to study the laser properties of the enhanced coupling device in the all-fiber system, three different InN samples have been analyzed for comparison purposes, namely S1, S2 and S3, with InN thickness = 1 µm, 360 nm, and 780 nm, respectively, showing exceptional nonlinear properties in the telecommunication region as demonstrated in previous reports [28]. Further details on the material growth and optical characterization of these samples can be found elsewhere [28]. To implement the SESAM, a 300 nm-thick aluminum layer was deposited on the InN film by radio-frequency sputtering at room temperature. The fiber laser is based on a simple ring-type cavity with the InN SESAM in reflection configuration. The whole system is based on single-mode fiber (SMFs), which ensures the stability of the laser and its immunity to vibrations or other external perturbation. The cavity comprises an erbium-doped fiber amplifier (EDFA, Accelink TV-series) as the gain medium with 16 m of Erbium-doped single-mode fiber (EDF). The EDF presents a 24 dBm gain and its group velocity dispersion (GVD) has been estimated in +16 ps^2/km at 1550 nm. Besides the active fiber and the SESAM, the oscillator consists of a conventional SMF, an isolator (ISO) and an optical coupler (OC) with 70/30 of coupling ratio. The laser output is taken at the 30% branch of the coupler. The length of the SMF is about 25 m, with a GVD of −21 ps^2/km at 1550 nm. Therefore, the effective dispersion of the EDF and SMF components are 0.256 ps^2 and −0.462 ps^2 respectively, resulting in a total dispersion of −0.21 ps^2 for the net cavity. Thus, the laser cavity behaves as a dispersion-managed laser cavity [35,36], operating in the anomalous dispersion regime. No polarization controller was inserted within the laser cavity due to the polarization independent wurtzite structure of the saturable absorber under normal-incidence illumination [37]. Therefore, any losses were inserted by the GRIN lens due to its polarization preservation property.

The laser output features are monitored using the following measurement equipment: an optical spectrum analyzer (Yokogawa AQ-6215B), a 4 GHz bandwidth oscilloscope (Keysight Technologies MSO9404A), a 32 GHz RF-spectrum analyzer (Agilent N9010A), a commercial autocorrelator (APE Mini PulseCheck), and an optical 1.5 GHz-photodetector (Thorlabs FPD310-FC-NIR).

The mode-locked fiber laser works in a self-starting configuration when pumped at maximum power (24dBm). Stable Gaussian stretched pulses without Kelly-sidebands were generated, as expected in strong dispersion-managed cavities [35]. However, when increasing the fiber length, higher harmonic generation would be produced, modifying the spectrum profile at the output of the laser cavity [38]. The pulse repetition rate of the oscillator was 5 MHz (Fig. 2(a)), which coincides with the fundamental mode configuration of the laser cavity (a time interval of 200 ns between consecutive pulses corresponds to the optical round trip of the fiber laser resonator). Figure 2(b) depicts a broadband measurement of the RF-pulse train (with a resolution bandwidth of 180 Hz and 1001 data points), which denotes the absence of parasitic disturbances, and thus the stability of the mode-locking. A signal to background ratio (SNR) of 42 dB was measured for the 14^{th} harmonic of the electrical spectrum as shown at the inset of Fig. 2(b) (acquired with a resolution bandwidth of 20 Hz and 10 kHz span, and a 0.1% of the output laser pulse in order to protect the detector from optical damage). No pedestal was observed in the RF spectrum, further confirming the mode-locking stability. To prove the stability of the proposed all-fiber assembly, a continuous monitoring measurement of the average power at the output of the laser cavity along

Optics EXPRESS

time was carried out, as depicted in Fig. 2(c). Output power was recorded every minute for a total of 60 hours of monitoring. As shown in Fig. 2(c), a slight increase in the optical power was measured with a standard deviation of 0.042 mW. The inset shows the optical spectrum of the pulse at the beginning and at the end of the monitoring measurement. This result indicates not only that the system has good stability but also that the SA device is suitable for prolonged use without generating any apparent damage.

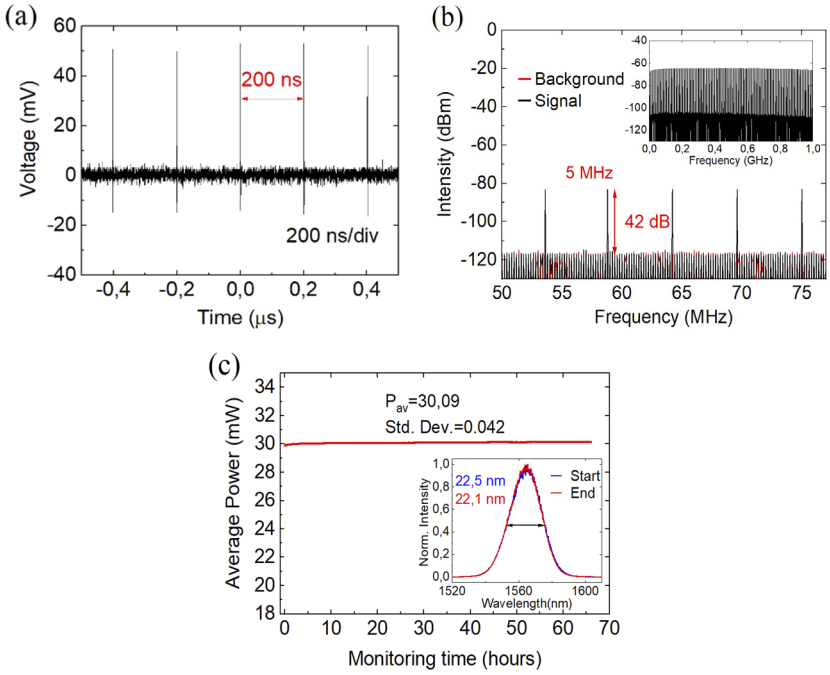

Fig. 2. Stability measurements of the pulse train: (a) mode-locked sequence as seen on the oscilloscope, (b) wide span measurement of the repetition rate, and (c) continuous monitoring of output power of the fiber laser as a function of time.

As discussed in previous reports [24,25], InN saturable absorbers have so far demonstrated excellent performances for laser mode-locking, including an enormous nonlinear response measured by the Z-scan technique (higher than 700% of nonlinear transmission change), broad modulation depths (up to 30%), and huge damage threshold levels (the maximum achievable optical peak-power by this type of system was registered in 1 MW [38]). Therefore, different samples (S1, S2, and S3) were implemented in this configuration (attached to the GRIN lens coupling device) and analyzed in terms of temporal duration and optical output power.

In order to obtain the mode-locked operation of the all-fiber laser system, the resonator was pumped at the maximum power of the EDFA in all cases. The autocorrelation trace of the generated pulses is depicted in Fig. 3(a), showing a pulse duration of 160 fs for S1, 94 fs for S2, and 92 fs for S3. The difference in temporal duration between the samples can be explained by the enhancement of the saturable absorption coefficient ($\alpha_2 = -3.5 \times 10^3$, -3×10^4, and -2.7×10^4 cm/GW for samples S1, S2, and S3, respectively) owing to the reduction of the residual carrier concentration (Burstein-Moss effect) [28]. The optical spectrum for each sample is shown in Fig. 3(b). The pulses were centered at 1564 nm (FWHM = 20.4 nm), 1570 nm (FWHM = 39.4 nm), and 1576 nm (FWHM = 42 nm) for S1, S2 and S3, respectively. The red shift observed for S2 and S3 with respect to S1 is due to their bandgap energy properties, as described in [28]. A Gaussian fitting function has been applied to the recorded data (black line).

Optics EXPRESS

While the shapes of the generated spectra unambiguously indicate the stretched pulse regime, the estimated overall dispersion seems to indicate the soliton mode-locked operation mode. This is very likely related to the limited knowledge of the exact amplifier dispersion value. The average power, peak power and pulse energy at the maximum pumping level were 40 mW, 50 kW, and 8 nJ for S1, 35 mW, 74.4 kW and 7 nJ for S2, and 30 mW, 65.2 kW and 6 nJ for S3, respectively. The time-bandwidth product (TBP) for each sample was calculated as 0.445 for S1, 0.45 for S2, and 0.46 for S3. It is worth noting that these TBP values are close to the theoretical value of 0.44 for a Gaussian pulse, which denotes a slight chirp of the optical pulses within the laser cavity.

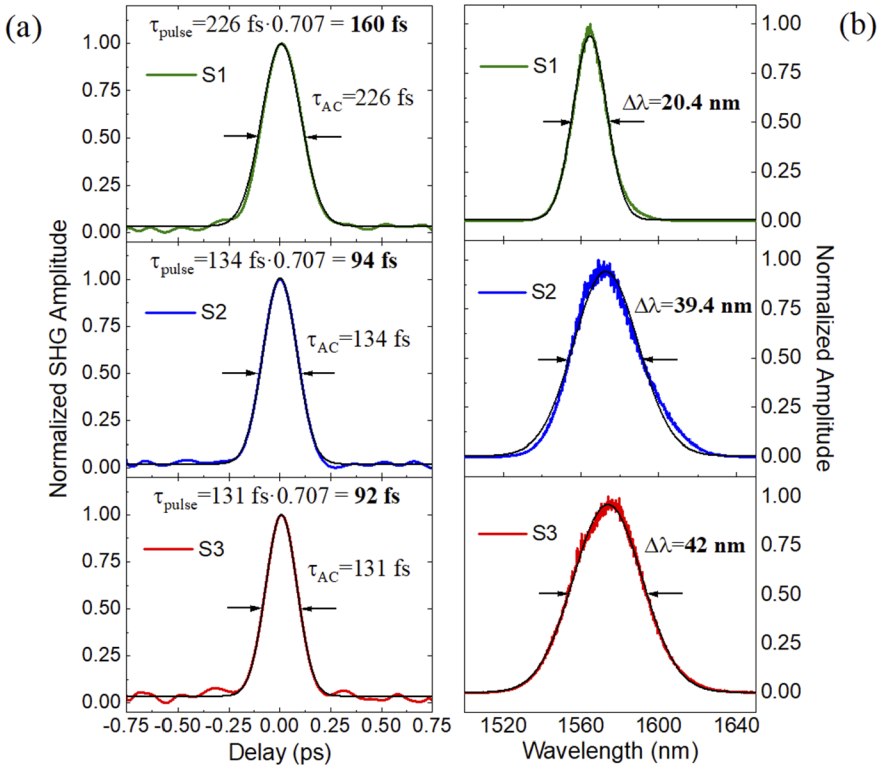

Fig. 3. Optical characterization of the output pulses: (a) autocorrelation trace with the corresponding Gaussian fit (black line) and (b) optical spectrum with the corresponding Gaussian fit (black line) for each sample.

By eliminating the optical aberrations and the defocusing behavior of free-space configurations, we obtain a reduction of the insertion losses within the laser cavity (5 dB of insertion losses compared to 8,5 dB in free-space configuration). Thereby, a higher intensity is achieved at the saturable absorber, thus increasing its nonlinear transmission change. This yields pulses with higher optical peak powers and shorter temporal widths. A reduction in the pulse duration (92 fs) is achieved in comparison to free-space cavity schemes reported in previous works as illustrated in Table 1 (with a temporal-width of 220 fs in transmission configuration and 134 fs with a reflection assembly [26,28]). In comparison to previous reports, the optical spectrum bandwidth increases by 35%, without any apparent deformation related to pulse breaking, denoting the stability of the mode-locked operation. At the same time, the pulse duration is reduced by 40% as shown in Table 1. Therefore, the introduction of the GRIN coupling device enhances the pulse focusing on the InN-based active layer, thereby increasing the induced nonlinear effect. This effect leads to a shortening of the temporal width of the pulse, while at the same time

Optics EXPRESS

maintaining its stability. Such a pulse duration of 92 fs was found to be among the shortest values that can be generated by a saturable absorber using an Er-doped fiber laser ring cavity without post-amplification [22]. On the other hand, the peak power and the energy increased by a factor of 3 due to the pulse compression (74 kW and 8 nJ in this work, to be compared to 28 kW and 5.4 nJ in latest results [28]). It is remarkable that the peak pulse energy is higher than those reported for 2D-based SAs [19,20,21,22]. These results indicate that the InN SA coupling device has unique advantages not only in the generation of ultrashort pulses, but also in the optimization of laser stability.

Table 1. Summary of autocorrelation and optical spectrum results for S1, S2 and S3 attached to a GRIN lens (GRIN) compared to free-space configuration (Air) in reflection mode laser cavity and their respective peak powers.

	AC Temporal duration (fs)		Spectral FWHM (nm)		Peak power (kW)	
Samples	Air[a]	GRIN	Air[a]	GRIN	Air[a]	GRIN
S1	190	160	19	20.4	24	50
S2	156.3	94	26.4	39.4	25.5	74.4
S3	134.4	92	40	42	28.2	65.2

[a]From Appl. Sci. **10**, 7832 (2020) [28].

3. Conclusion

In summary, we have demonstrated an all-fiber mode-locked laser operating in the telecommunication spectral range by incorporating an InN-based SESAM integrated with a GRIN-rod lens as a coupling device. This compact, polarization independent and alignment-free assembly can deliver highly stable ultrafast laser pulses at 1.56 µm, with a temporal duration as short as 90 fs. The reduced overall losses of this arrangement compared to free-space configurations (3.5 dB) leads to high-energy output pulses with a peak power of 74 kW and an energy of 8 nJ without damaging the InN saturable absorber. Overall, the optimized InN SA (with properties such as high modulation depth (up to 30%), high nonlinear transmission change (700%) and high damage threshold) attached to the GRIN lens has the potential to be exploited as a simple coupling device for ultra-stable mode-locked lasers which may open the path for commercial applications.

Funding. Ministerio de Ciencia, Innovación y Universidades (RTI2018-097957-B-C31); Comunidad de Madrid (S2018/NMT-4326).

Disclosures. The authors declare no conflicts of interest.

Data availability. Data underlying the results presented in this paper are available in Ref. [39].

References

1. K. Sugioka and Y. Cheng, "Ultrafast lasers—reliable tools for advanced materials processing," Light: Sci. Appl. **3**(4), e149 (2014).
2. J. Cheng, C. Liu, S. Shang, D. Liu, W. Perrie, G. Dearden, and K. Watkins, "A review of ultrafast laser materials micromachining," Optics & Laser Tech. **46**, 88–102 (2013).
3. S. Taccheo, "Fiber lasers for medical diagnostics and treatments: state of the art, challenges and future perspectives," Proc. SPIE **10058**, 1005808 (2017).
4. W. H. Knox, "Ultrafast technology in telecommunications," IEEE J. Select. Topics Quantum Electron. **6**(6), 1273–1278 (2000).
5. M. N. Zervas and C. A. Codemard, "High Power Fiber Lasers: A Review," IEEE J. Select. Topics Quantum Electron. **20**(5), 219–241 (2014).
6. M. W. Phillips, A. I. Ferguson, D. C. Hanna, M. J. McCarthy, and P. J. Suni, "Actively Mode-Locked Fiber Lasers," Proc. SPIE 1171, (1990).
7. D. D. Hudson, K. W. Holman, R. J. Jones, S. T. Cundiff, J. Ye, and D. J. Jones, "Mode-locked fiber laser frequency-controlled with an intracavity electro-optic modulator," Opt. Lett. **30**(21), 2948–2950 (2005).
8. E. Garmire and A. Yariv, "Laser mode-locking with saturable absorbers," IEEE J. Sel. Top. Quantum Electron. **3**(6), 222–226 (1967).

Optics EXPRESS

9. U. Keller, "Recent developments in compact ultrafast lasers," Nature **424**(6950), 831–838 (2003).
10. X. M. Liua, T. Wanga, C. Shub, L. R. Wanga, A. Lina, K. Q. Lua, T. Y. Zhanga, and W. Zhao, "Passively harmonic mode-locked erbium-doped fiber soliton laser with a nonlinear polarization rotation," Laser Phys. **18**(11), 1357–1361 (2008).
11. A. V. Avdokhin, S. V. Popov, and J. R. Taylor, "Totally fiber integrated, figure-of-eight, femtosecond source at 1065 nm," Opt. Express **11**(3), 265–269 (2003).
12. K. Yin, Y. Li, Y. Wang, X. Zheng, and T. Jiang, "Self-starting all-fiber PM Er:laser mode locked by a biased nonlinear amplifying loop mirror," Chin. Phys. B **28**(12), 124203 (2019).
13. U. Keller, K. J. Weingarten, and F. X. Kartner, "Semiconductor saturable absorber mirrors (SESAM's) for femtosecond to nanosecond pulse generation in solid-state lasers," IEEE J. Sel. Top. Quantum Electron. **2**(3), 435–453 (1996).
14. A. Autere, H. Jussila, Y. Dai, Y. Wang, H. Lipsanen, and Z. Sun, "Nonlinear optics with 2D layered materials," Adv. Mater. **30**(24), 1705963 (2018).
15. M. Houssa, A. Dimoulas, and A. Molle, *2D Materials for Nanoelectronics*, 1st Ed. (CRC Press, 2016).
16. K. Kostarelos, "Translating graphene and 2D materials into medicine," Nat. Rev. Mater. **1**(11), 16084 (2016).
17. J. Sotor, I. Pasternak, A. Krajewska, W. Strupinski, and G. Sobon, "Sub-90 fs a stretched-pulse mode-locked fiber laser based on a graphene saturable absorber," Opt. Express **23**(21), 27503–27508 (2015).
18. B. Fu, Y. Hua, X. Xiao, H. Zhu, Z. Sun, and C. Yang, "Broadband Graphene Saturable Absorber for Pulsed Fiber Lasers at 1, 1.5, and 2 μm," in *IEEE Journal of Selected Topics in Quantum Electronics*, 20(5), 411–415 (2014).
19. W. Liu, L. Pang, H. Han, W. Tiang, H. Cheng, M. Lei, P. Yan, and Z. Wei, "70-fs mode-locked erbium-doped fiber laser with topological insulator," Sci. Rep. **6**(1), 19997 (2016).
20. W. Liu, L. Pang, H. Han, M. Liu, M. Lei, S. Fang, H. Teng, and Z. Wei, "Tungsten disulfide saturable absorbers for 67 fs mode-locked erbium-doped fiber lasers," Opt. Express **25**(3), 2950–2959 (2017).
21. X. Jin, G. Hu, M. Zhang, Y. Hu, T. Albrow-Owen, R. C. T. Howe, T. Wu, Q. Wu, Z. Zheng, and T. Hasan, "102 fs pulse generation from a long-term stable, inkjet-printed black phosphorus-mode-locked fiber laser," Opt. Express **26**(10), 12506–12513 (2018).
22. M. Zhang, Q. Wu, F. Zhang, L. Chen, X. Jin, Y. Hu, Z. Zheng, and H. Zhang, "2D Black Phosphorus Saturable Absorbers for Ultrafast Photonics," Adv. Opt. Mater. **7**(1), 1800224 (2019).
23. J. Du, M. Zhang, Z. Guo, J. Chen, X. Zhu, G. Hu, P. Peng, Z. Zheng, and H. Zhang, "Phosphorene quantum dot saturable absorbers for ultrafast fiber lasers," Sci. Rep. **7**(1), 42357 (2017).
24. B. Guo, S. Wang, Z. Wu, Z. Wang, D. Wang, H. Huang, F. Zhang, Y. Ge, and H. Zhang, "Sub-200 fs soliton mode-locked fiber laser based on bismuthene saturable absorber," Opt. Express **26**(18), 22750–22760 (2018).
25. M. Jiménez-Rodríguez, E. Monroy, and M. González-Herráez, and F.B. Naranjo, "Ultrafast fiber laser using InN as saturable absorber mirror," J. Lightwave Technol. **36**(11), 2175–2182 (2018).
26. L. Monroy, M. Jiménez-Rodríguez, P. Ruterana, E. Monroy, M. González-Herráez, and F. B. Naranjo, "Effect of the residual doping on the performance of InN epilayers as saturable absorbers for ultrafast lasers at 1.55μm," Opt. Mater. Express **9**(7), 2785–2792 (2019).
27. J. Wu, W. Walukiewicz, K. M. Yu, J. W. Ager, E. E. Haller, H. Lu, W. J. Schaff, Y. Saito, and Y. Nanishi, "Unusual properties of the fundamental band gap of InN," Appl. Phys. Lett. **80**(21), 3967–3969 (2002).
28. L. Monroy, M. Jiménez-Rodríguez, E. Monroy, M. González-Herráez, and F. B. Naranjo, "High-Quality, InN-Based, Saturable Absorbers for Ultrafast Laser Development," Appl. Sci. **10**(21), 7832 (2020).
29. A. Reina, H. B. Son, L. Y. Jiao, B. Fan, M. S. Dresselhaus, Z. F. Liu, and J. Kong, "Transferring and identification of single- and few-layer graphene on arbitrary substrates," J. Phys. Chem. C **112**(46), 17741–17744 (2008).
30. S. Yamashita, Y. Inoue, S. Maruyama, Y. Murakami, H. Yaguchi, M. Jablonski, and S. Y. Set, "Saturable absorbers incorporating carbon nanotubes directly synthesized onto substrates and fibers and their application to mode-locked fiber lasers," Opt. Lett. **29**(14), 1581–1583 (2004).
31. A. Martinez, M. Al Araimi, A. Dmitriev, P. Lutsyk, S. Li, C. Mou, A. Rozhin, M. Sumetsky, and S. Turitsyn, "Low-loss saturable absorbers based on tapered fibers embedded in carbon nanotube/polymer composites," APL Photonics **2**(12), 126103 (2017).
32. J. Zhao, S. Ruan, P. Yan, H. Zhang, Y. Yu, H. Wei, and J. Luo, "Cladding-filled graphene in a photonic crystal fiber as a saturable absorber and its first application for ultrafast all-fiber laser," Opt. Eng. **52**(10), 106105 (2013).
33. S. Ko, J. Lee, J. Koo, B. S. Joo, M. Gu, and J. H. Lee, "Chemical wet etching of an optical fiber using a hydrogen fluoride-free solution for a saturable absorber based on the evanescent field interaction," J. Lightwave Technol. **34**(16), 3776–3784 (2016).
34. B. Guo, X. Guo, L. Tang, W. Yang, Q. Chen, and Z. Ren, "Ultra-long-period grating-based multi-wavelength ultrafast fiber laser [Invited]," Chin. Opt. Lett. **19**(7), 071405 (2021).
35. K. Tamura, E. P. Ippen, H. A. Haus, and L. E. Nelson, "77-fs pulse generation from a stretched-pulse mode- locked all-fiber ring laser," Opt. Lett. **18**(13), 1080–1082 (1993).
36. S. K. Turitsyn, B. G. Bale, and M. P. Fedoruk, "Dispersion-managed solitons in fibre systems and lasers," Phys. Rep. **521**(4), 135–203 (2012).
37. M. Jimenez-Rodriguez, L. Monteagudo-Lerma, E. Monroy, M. González-Herráez, and F. B. Naranjo, "Widely power-tunable polarization-independent ultrafast mode-locked fiber laser using bulk InN as saturable absorber," Opt. Express **25**(5), 5366–5375 (2017).

Optics EXPRESS

38. F. Gallazzi, M. Jimenez-Rodriguez, E. Monroy, P. Corredera, M. González-Herráez, F. B. Naranjo, and J. D. A. Castañón, "Sub-250 fs passively mode-locked ultralong ring fibre oscillators," Opt. Laser Technol. **138**, 106848 (2021).
39. L. Monroy, "Analysis of an ultrafast all-fiber laser based on InN-GRIN SESAM," e-cienciaDatos, July 2021, https://doi.org/10.21950/BJL0KT.